RSC Advances

ROYAL SOCIETY
OF CHEMISTRY

www.rsc.org/advances

Journal Name

ARTICLE

RSC Advances Accepted Manuscript

A novel preparation for PVA/ L-Histidine/AgNPs membrane and its antibacterial property

Zhiqiang Cheng‡[a,b], Fanli Zhang‡[a], Wei Liu[a] , Lijuan Kang*[a], Liying Cui[a]

In this paper, we have firstly prepared an antibacterial material of PVA/L-histidine(L-H)/Ag fibers by electrospinning in double nozzle. The composite fibers were crosslinked by the mixture of glutaraldehyde and hydrogen chloride gas. After that, it was characterized by transmission electron microscopy (TEM), scanning electron microscopy (SEM), Energy Dispersive X-ray Spectroscopy (EDS) and FT-IR spectra. The results indicated the size of silver particle distributed on the fiber was in nanoscale below the 10 nm, and OH groups have significantly decreased but the C=O groups increased after treatment of the crosslinked by gas phase. Simultaneously, the mechanical property for the membrane also have greatly improved and the maximum strain and toughness reached to 225.01% and 11.31 J g^{-1} respectively . At last, in order to investigate the antibacterial property of the membrane, we choosed E. coli and Staphylococcus as inhibition target, which showed the excellent antibacterial property for blocking the growth and destroying the structure of the bacteria.

Introduction

Electrospinning has attracted lots of attention in the academic research and industrial production,[1] since it is very simple, low-cost, and effective technology to produce ultrafine fibers which exhibit outstanding properties with high specific surface area and large volume-to-mass ratios.[2] In the past years, electrospinning materials have been applied in the wound dressing,[3,4] separation filters,[5, 6, 7] tissue scaffold,[8] sensors,[9] as well as energy area,[10-12] catalysts[13, 14] and reinforced composites.[15, 16] However, there has been considerable interest in the biomedical field.[17-19] As we know that infections which develop in traumatic and surgical wounds remain a major problem for threatening the health of patients. One of the key approaches for minimizing the possibilities of wound infections is the application of topical antimicrobial agents.[20] To solve the problem of the antimicrobial properties of medicinal materials, silver is a widely-used and recognized broadspectrum biocidal agent that is effective against bacteria, fungi and viruses but is non-toxic to human cells.[3] In the recent years, electrospun nanofibers with silver have attracted interest as a novel form of antimicrobial material.[21-23] Insertion of Ag nanoparticles into different polymer matrixes will cause dramatic improvement of the properties and there are some reports on the preparation and properties of polymer-Ag nanoparticle composite nanofibers. However, nanofibers containing silver

by the traditional process has demonstrated reduced antimicrobial efficiency due to Ag nanoparticle aggregation and subsequent reduced bioavailability.[3, 24] In situ reduction of silver ions in electrospinning fibers results in a more uniform dispersion of Ag nanoparticles under suitable situations,[25-27] such as UV light, γ-rays, ultrasound, prolonged reflux or chemicals.[23, 28-30] Silver antibacterial agents belong to the inorganic antibacterial agent, which can overcome the many drawbacks of organic antibacterial agents and due to the properties of high security performance, strong persistence, the advantages of high heat resistance, high antibacterial performance, it has been used in antimicrobial building materials, textile, ceramics and coatings widely.[31-32]

This paper firstly reports on a novel and efficient method that uses double tube electrostatic spinning nozzle which has been patented for our own to produce PVA/L-histidine/AgNO$_3$ hybrid nanofibers. L-histidine is one of necessary amino acids for the people, which plays great role in repairing the injured tissues, and it is beneficial to enhance and assist in the healing of ulceration and allergy. Meanwhile, PVA is a semi-crystalline hydrophilic polymer with good chemical and thermal stability[33] and it has been used especially in fiber and film products for many years. Also, it is highly biocompatible and non-toxic,[34, 35] easy for degradation in the environment by microorganism and without secondary pollution.[36, 37] It can be processed easily and has high water permeability. These properties have led to the use of PVA in a wide range of applications in medical, cosmetic, food, pharmaceutical, and packaging industries.[38] For most polymer solutions with Silver ions, the silver ions would be unstable and easy to decompose, which has put a hard squeeze for the production and property of fibers. Therefore, we firstly prepared composite ultrafine fibers containing silver with PVA and histidine by

[a] College of Resources and Environment, Jilin Agriculture University, Changchun 130118, People's Republic of China
[b] School of Aerospace Engineering, Tsinghua University, Beijing, 100000, China.
* Corresponding author   E-mail: kanglijuan61@126.com
‡ Fanli Zhang and Zhiqiang Cheng contributed to the work equally.
† Electronic supplementary information (ESI) available. See DOI: 10.1039/x0xx00000x

electrospinning tech technique in special electrospinning needle, which could avoid prolonged contact of PVA and silver. As we knew the fact that the coordination of the amino acid to silver (I) ion seems to occur through the amino-group or carboxy group, forming two or four coordinate complexes.[39] So, L-histidine refers as the Stabilizer for the Silver during the process. Concrete process was discussed in the ESI (Figure S1, ESI†). For the biological compatibility of PVA, it is the support plates and easy for histidine to adhere on the surface of PVA. Although many types of nanofibers containing silver were prepared using electrospinning technique, PVA/L-histidine nanofibers with nanoparticles of Ag has not been prepared yet. Furthermore, this article demonstrates the effectiveness of the PVA/L-h/Ag nanofiber mats on antibacterial performance, excellent tensile strength after treatment of gas-crosslinked by glutaraldehyde, which provides a mild avenue to develop a new preservative. The surface and bulk morphologies and antibacterial effectiveness and duration of the resultant PVA/L-h/AgNO$_3$ hybrid nanofibers were systematically investigated.

Experimental section

Materials

Polyvinyl alcohol 1799 (PVA, alcoholysis: 99.8%~100%) was purchased from Aladdin. L-histidine was purchased from Beijing BioDee Biotechnology co. Ltd. Silver nitrate (AgNO$_3$, AR) and formic acid (HCOOH) were obtained from the Sinopharm chemical reagent co. Ltd. Hydrochloric acid (HCl, 36%~38%) and Glutaraldehyde (C$_5$H$_8$O$_2$, 25%) were purchased from Beijing Chemical Works. Ultrapure water was used in all experiments. All chemicals were used without further purification.

Methods

Firstly, 5ml formic acid (Reducing agent for silver) and the 16ml Uw were mix thoroughly at the volume ratio of 1:3.2. A certain amount of PVA was dissolved in the solution at 80 ℃ under magnetic stirring for 4 h and the mass percentage concentrations were 12%, 14%, 16% respectively. The PVA solution was put in tube A as shown in the Fig.1. Secondly, 0.47g AgNO$_3$ was mixed in the 10ml saturated solution of L-histidine (4.3/100 ml, 25 ℃) at the molar ratio of 1:1 in room temperature and reacted for 1h stiring slightly. Simultaneously, the AgNO$_3$/L-h solution was put in the tube B. Finally, the two liquids would flow by the gravity. During the electrospinning process, we control the flow rate via adapting the slants of the electrospinning jet. The high voltage of 20 kV was applied and the distance from needle-tip to acceptor connected with the ground wire was 20 cm. The as-spun PVA/L-h/Ag membranes were gas-cross-linked by glutaraldehyde (Roles for crosslinking agent and reducing agents) in drying apparatus for 3h at room temperature. The crosslinked films were dried for 24 h in vacuum drier at 30 ℃ to remove residual solvents.
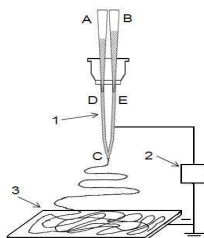

Figure 1: the schematic diagram of electrostatic spinning equipment (1 Copper tube, 2 High Voltage Supplier, 3 Acceptor)

Characterizations and measurements

The X-ray diffraction (XRD) patterns of the sample was measured using a D/MAX 2250 V diffractometer (Rigaku, Japan), using Cu Kα (λ = 0.15418 nm) radiation under 40 Kv, 30 mA and scanning over the range of 10° to 90°. Surface morphology of nanofibers was observed using Scanning Electron Microscope (SEM, SHIMADZU X-550) after applying a gold coating, Scanning Transmission Electron Microscopy (STEM, Tecnai G2), Transmission Electron Microscopy (TEM, Tecnai G2). Fourier transform infrared (FTIR) spectra of the samples were obtained using a Paragon 1000 Spectrometer (Perkin Elmer) at a signal resolution of 1 cm^{-1} within the range of 400~4000 cm^{-1}. The micro-screw meter (0-25, Shanghai) was applicated for measuring the thickness of membrane directly. The mechanical property was measured by Fibre tensile tester (WDW-X) with stretching velocity of 5mm/min. Elemental analysis was carried out by Energy Dispersive X-ray Spectroscopy (EDS). The UV–vis spectrophotometer (Hitachi U-3010) was used for measuring the optical density (OD) of bacterial broth medium at 600 nm.

Antibacterial assessment assay

The antibacterial efficacy of PVA/L-H/Ag nanofibers was evaluated by using E. coli and Staphylococcus aureus. Bacterial inoculum was prepared in Tryptic Soy broth (medium pH 7.3) containing 17 g/L Pancreatic Digest of Casein, 3 g/L Papaic Digest of Soybean, 2.5 g/L Dextrose, 5 g/L NaCl and 2.5 g/L Dipotassium phosphate. The solid medium was solidified by 10 g L^{-1} agar.

For antibacterial assessment, 50 μL of bacterial solution with about 10^6 CFU mL^{-1} of E. coli and Staphylococcus aureus were dispensed onto an agar plate respectively, and then crosslinked PVA/L-H/AgNPs sample (1cm × 1cm) was covered on the surface of the plates. After incubation for 24 h at 37 ℃, the bacterial growth inhibition halos were observed. The crosslinked PVA/L-H membrane was used as controls with containing silver particles sample.

Owing to studying the antibacterial kinetics of the samples, the 10 mg crosslinked fibers of PVA, PVA/L-H, PVA/L-H/AgNPs were added into 50 mL bacteria nutrient solution respectively with the concentration of E. coli for 10^4 CFUmL^{-1}. Bacteria nutrient solution with the same concentration was incubated at the same condition and used as control. The optical density (OD) of bacterial broth medium at 600 nm was measured by UV–vis spectrophotometer.

Results and discussion

Figure 2 provides the scanning electron microscopy, transmission electron microscopy and scanning transmission electron microscopy images of composite fibers. It shows that the concentration of PVA plays an important role in the diameter and uniformity of the composite fibers of PVA/L-H/Ag. As the pictures showed that, 14% PVA kept the good microscopy among the three concentrations of 12%, 14% and 16%. When the concentration of PVA added to 16%, the fibers would occur clinging with ambient fibers for the hardness of

volatilization. The Ag nanoparticles (AgNPs) were formed preferentially on the surface of the PVA/L-H/Ag fiber from the TEM and STEM images. As we know that Ag particles with sizes of 1-10nm could destroy the permeability and respiratory functions of bacteria.[40] The Figure 2D shows that the diameter of the AgNPs ranged from 0.1 nm to 8.7 nm and and their size distribution was very narrow on the composite fiber, so it would be good for antibacterial property. As we can see from the Fig. 2F, the EDX mapping results confirm the presence of Ag, O, and C elements in the membrane, which reveals the capacity of metallic Ag in the composite fibers. These results indicate that glutaraldehyde successfully reduced the Ag^+ and that L-histidine as a stabilizing agent inhibiting the agglomeration of the Ag nanoparticles followed crosslinked process. Thereby, it can efficiently inactivate the growth of bacteria.
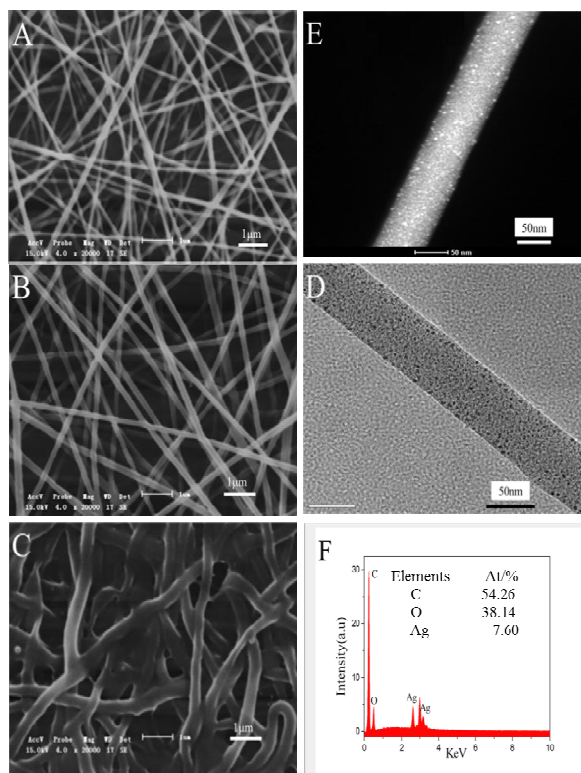

Figure 2: SEM (A-C) micrograph of fibers electrospun from PVA/L-h/Ag containing different content of PVA (12%, 14%, 16%); D-E TEM and STEM of the (14% PVA) PVA/L-h/Ag fiber; F the EDS spectrum of (14% PVA) PVA/L-h/Ag membrane.
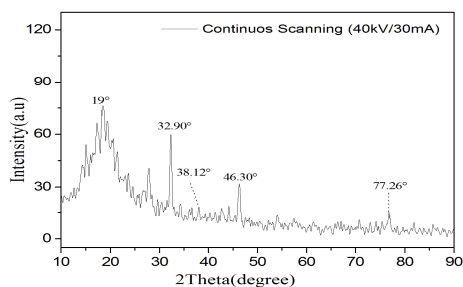

Figure 3: The XRD pattern of PVA/L-H/AgNPS membrane

The XRD pattern of PVA/L-H/AgNPs nanocomposite membrane is shown in Fig. 3. As shown in the pattern, there are some peaks around 20°, which can be assigned to PVA and L-histidine. According to the diffraction peaks, we can confirm the mode of existence for silver. 2θ= 38.90° and 77.26° are the typical diffraction peaks of silver, but there are some diffraction peaks for Ag_2O in the pattern, such as 32.90°, 46.30° , because the silver ions would be oxidized during electrospinning process. Simultaneously, the peaks around 20° were edge sharping. The addition of $AgNO_3$ might improve the crystallinity of PVA, this is because the silver nitrate in the reaction have played an important role in heterogeneous nucleation, increase the crystallization properties of PVA.[41]

Fourier Transform Infrared Spectroscopy (FT-IR) was used to characterize the presence of specific chemical groups in the materials. As the image shows that, the FT-IR spectra of crosslinked PVA/L-h/AgNPs have some changes comparing to that of original membrane. The large bands around 3350 cm^{-1} are corresponding to the stretching O–H from the intermolecular and intramolecular hydrogen bonds.[42] After the vapor crosslinking, the intensity of O–H group was observed relatively decreasing when compared to the original film of PVP/L-h/AgNPs. The vibrational band near the 2940 cm^{-1} refers to the stretching C–H. The peaks around 1728 cm^{-1} are linked to the stretching C=O and C-O from PVA and the intensity increased after crosslinking.[43] The band observed at 1000–1140 cm^{-1} with gradual broadening of the peak width after crosslinking is attributed to O-C-O vibration of the acetal group.[44] The mechanical property of the membrane enhanced greatly after crosslinking, which was significantly related to the new formation of specific chemical groups. Generally, the crosslinking degree of the membrane has an influence on the property of water absorbency. The detail was discussed in ESI (Fig. S2. ESI †).

Figure 4: the contrast of FTIR of crosslinked PVA/L-h/Ag and uncrosslinked films (A Original membrane, B crosslinked membrane)
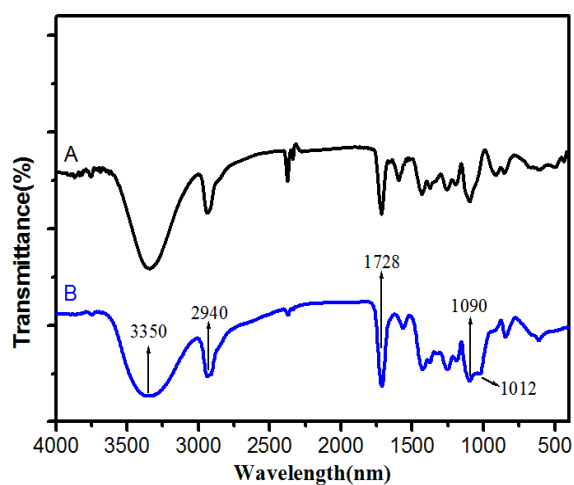
Table 1 : the mechanical properties of PVA/L-h/AgNPs Nanofibers in Tensile Load

| Crosslink time/h	E modulus (M Pa)	Stress (M Pa)	Strain Break (%)	Thickness (mm)	Toughness (J g^{-1})	Area (M Pa)	Density (g cm^{-3})
2	5.53 ± 2.21	3.67 ± 0.95	86.3 ± 2.0	0.06 ± 0.002	2.02 ± 0.4	2.31 ± 0.23	1.15 ± 0.06
3	4.43 ± 0.54	7.22 ± 0.36	149.2 ± 7.9	0.06 ± 0.001	5.58 ± 0.7	6.69 ± 0.19	1.20 ± 0.03
4	2.55 ± 0.79	5.40 ± 0.51	204.6 ± 11.2	0.09 ± 0.007	5.84 ± 0.5	7.19 ± 0.45	1.23 ± 0.11
5	4.25 ± 0.86	11.12 ± 1.01	225.1 ± 2.8	0.07 ± 0.003	10.99 ± 0.9	14.73 ± 1.12	1.34 ± 0.10
6	9.04 ± 1.02	15.01 ± 0.53	183.4 ± 2.3	0.08 ± 0.002	11.31 ± 0.7	15.27 ± 1.32	1.35 ± 0.07
7	2.46 ± 0.36	4.07 ± 0.23	169.3 ± 1.5	0.08 ± 0.003	2.83 ± 0.3	3.79 ± 1.04	1.34 ± 0.02
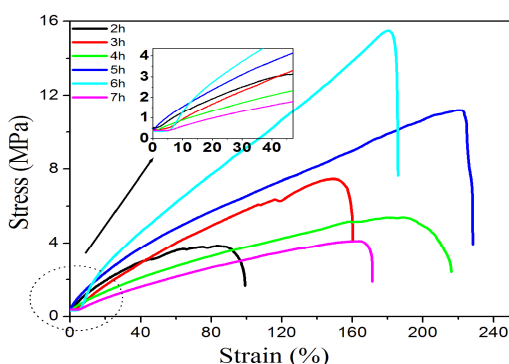
Figure 5 The stress–strain curves of crosslinked PVA/L-h/AgNPs nanofibers in tensile load

The mechanical property plays important role in the application for the material.[45] Fig. 5 shows the tensile strength response recorded for the PVA/L-h/AgNPs at different crosslinking time by the mixed gas atmosphere of hydrogen chloride and glutaraldehyde. With the crosslinking time increasing from 2h to 5h, the toughness of fibers gradually increased from 2.02 J g^{-1} to 11.31 J g^{-1}, and there were significant changing strain at break from 86.3% to 225.1%. The Table 1 indicated that the mechanical property of the membrane had great enhancement after treatment by crosslinking. The molecules would tie together and form the three-dimensional structure after crosslinking, therefore the drawing force not only break the bond of molecular internal forces, but also the forces of intermolecular and then the physical performance get increase[46,47]. However, the mechanical property would decrease after the further crosslinking. As the detailed data show in the Table 1, when the crosslinking time increased to 6h, the breaking stress reached 15.01MPa, but the strain of the membrane was reduced to about 183%. With the crosslinking time further continuing, the mechanical property of the films declined sharply. After the crosslinking time for 7 hours, the fracture stress fell to 4.07MPa and the breaking strain was reduced to 169.3%. This is mainly due to the excessive crosslinking, which leads to the brittleness change of the membrane[46]. It is easy to produce stress concentration due to the reduced toughness of membrane, which affects the overall mechanical properties of PVA/L-H/Ag nanofibers.

In this study, in order to investigate the antibacterial properties of PVA/L-H/AgNPs, The antibacterial capacities of the PVA/L-H/Ag nanofibers against Staphylococcus aureus and E. coli were explored by observing the inhibition halo of the bacterial. Figure 6(a) and (b) as crosslinked PVA/L-H films and crosslinking PVA/L-H/Ag membrane respectively show the bacteriostatic circle diagram of staphylococcus aureus. Simultaneously, figure 6(c), 6(d) are the crosslinked PVA/L-H and PVA/L-H/Ag membrane respectively for inhibition halo of E. coli. As we can see from the membranes in the petri dishes, the films containing silver were in light brown, the others are in white. The composite fibers with silver show the good antibacterial effect from the inhibition halo of E. coli and Staphylococcus aureus. There is no bacterial multiplication and bacterial growth around the membranes and the antibacterial length for E. coli and Staphylococcus aureus are 0.5cm and 1.1cm respectively. The reasons for the property of antibacterial are that the composite fibers have the advantage of the small size for absorbing on the bacterial cell walls by hydrogen bonding force and static electricity, which leads to inhibition action and blocking the growth of bacteria, then resulting in the death of them ultimately[48]. The other possibility is that PVA/L-H/Ag would get inside bacterial cells through diffusion and osmosis, and destroy the cell enzymes and protease, then kill the bacteria. The smaller of the Ag particles size, the easier for them to access to the inside of bacteria and kill it. By comparing the two pictures of Fig. 6b and Fig. 6d, the composite fibers showed high antibacterial efficiency for Staphylococcus aureus than E. coli. This is possible because that the size of the silver nanoparticles on the surface of composite fibers is similar to that of staphylococcus aureus[49], therefore, it is more easily to get the interior of the bacteria and prevent the growth of bacteria and kill the bacteria finally. Meanwhile, we also studied the antibacterial kinetics against E. coli, which part was discussed detailedly in the ESI (Fig. S3, ESI†). The membrane showed significantly antibacterial ability in the incubation process,

therefore, the PVA/L-H/AgNPs nanofibers have the potential to be utilized as antibacterial biomaterials.
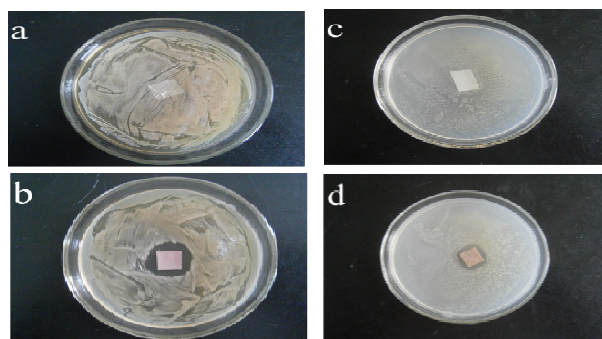
.Figure 6: the bacterial growth inhibition halos against Staphylococcus aureus for PVA/L-h (a) and PVA/L-H/Ag (b) nanofibers; the bacterial growth inhibition halos against E. coli for PVA/L-H(c) and AgPVA/L-H/Ag (d) nanofibers.

Conclusions

Antibacterial membrane of PVA/L-h/AgNPs was prepared by electrospinning technique in our own approach. We have confirmed the optimal by adjusting the experimental parameters. Moreover, the gaseous mixture of hydrochloric acid and glutaraldehyde provided the reducing agent for silver ions to Ag as well as cross-linking agent for composite fibers of PVP/L-h during the process of treatment, which strengthen the mechanical properties of composite fibers. During the experiments of inhibition for the bacteria, the PVA/L-H/AgNPs showed excellent antibacterial property for inhibiting growth of the microorganisms of S. aureus and E. coli from the inhibition halos. Duo to the character of porosity around the fibers, this study demonstrated convenient and cost-effective approach to develop antimicrobial membranes that would have great potential for the applications of the filtration of water or air in the future.

Acknowledgements

References

1. L. Dan, Y. Xia. *Advanced materials* , 2004, **16**, 1151

2. M. A. Shannon, P. W. Bohn, M. Elimelech, J. G. Georgiadis, B. J. Mariñas, A. M. Mayes, *Nature*, 2008, **452**, 301

3. Q. Shi, N. Vitchuli, J. Nowak, J. M. Caldwell, F. Breidt, M. Bourham, M. McCord, *European polymer journal*, 2011, **47** 1402

4. P. O. Rujitanaroj, N. Pimpha, P. Supaphol, *Polymer*, 2008, **49** 4723

5. S. Kaur, S. Sundarrajan, D. Rana, R. Sridhar, R. Gopal, T. Matsuura, S. Ramakrishna, *Journal of Materials Science*, 2014, **49**, 6143

6. Z. Xue, Y. Cao, N. Liu, L. Feng, L. Jiang, *J. Mater. Chem. A,* 2014, **2**, 2445

7. M. W. Lee, S. An, S. S. Latthe, C. Lee, S. Hong, S. S. Yoon, *ACS applied mater. Interfaces*, 2013, **5**, 10597

8. A. Gupta, A. M. Seifalian, Z. Ahmad, M. J. Edirisinghe, M. C. Winslet, *Journal of bioactive and compatible polymers*, 2007, **22**, 265

9. I. D. Kim, A. Rothschild, B. H. Lee, D. Y. Kim, S. M. Jo, H. L. Tuller, *Nano Letters*, 2006, **6,** 2009

10. V. Thavasi, G. Singh, S. Ramakrishna, *Energy Environ. Sci.,* 2008, **1**, 205

11. W. Xu, Y. Ding, S. Jiang, L. Chen, X. Liao, H. Hou, *Materials Letters,* 2014, **135**, 158

12. S. Cavaliere, S. Subianto, I. Savych, D. J. Jones, J. Rozière, *Energy Environ. Sci.,* 2011, **4**, 4761

13. A. C. Patel, S. Li, C. Wang, W. Zhang, Y. Wei, *Chem. Mater.,* 2007, **19**, 1231

14. X. Peng, W. Ye, Y. Ding, S. Jiang, M. Hanif, X. Liao, H. Hou, *RSC Adv.,* 2014, **4**, 42732

15. A. Zucchelli, M. L. Focarete, C. Gualandi, S. Ramakrishna, *Polymers for Advanced Technologies*, 2011, **22**, 339

16. S. Jiang, A. Greiner, S. Agarwal, *Compos. Sci. Technol.,* 2013, 87, 164

17. S. Agarwal, J. H. Wendorff, A. Greiner, *Polymer*, 2008, **49,** 5603

18. D. Kai, S. S. Liow, X. J. Loh, *Materials Science and Engineering: C*, 2014, **45**,659

19. P. Ke, X. N. Jiao, X. H. Ge, W. M. Xiao and B. Yu, *RSC Adv.,* 2014, **4**, 39704

20. M. A. Davoodbasha, S. Y. Lee, S. C. Kim and J. W. Kim, *RSC Adv*., 2015, **5**, 35052

21. W. K. Son, J. H. Youk, T. S. Lee, W. H. Park, *Macromolecular rapid communications*, 2004, **25**, 1632

22. P. O. Rujitanaroj, N. Pimpha, P. Supaphol, *Polymer*, 2008, **49**, 4723

23. H. K. Lee, E. H. Jeong, C. K. Baek, J. H. Youk, *Materials Letters*, 2005, **59**, 2977

24. H. J. Jeon, J. S. Kim, T. G. Kim, J. H. Kim, W. R. Yu, J. H. Youk, *Applied Surface Science*, 2008, **254**, 5886

25. W. K. Son, J. H. Youk, W. H. Park, *Carbohydrate Polymers*, 2006, **65**, 430

26. F. Zhang, Z. Cheng, L. Kang, L. Cui, W. Liu, X. Xu, G. Hou, H. Yang, *RSC Adv*., 2015, **5**, 32088

27. A. M. Abdelgawad, S. M. Hudson, O. J. Rojas, *Carbohydrate polymers*, 2014, **100**, 166

28. I. Díez, R. H. Ras, *Nanoscale*, 2011, **3**, 1963

29. P. Chen, L. Song, Y. Liu, Y. E. Fang, *Radiation Physic and Chemistry*, 2007, **76**, 1165

30. V. G. Pol, D. N. Srivastava, O. Palchik, V. Palchik, M. A. Slifkin, A. M. Weiss, A. Gedanken, *Langmuir*, 2002, **18**, 3352

31. I. Tsyba, B. B. K. Mui, R. Bau, R. Noguchi, K. Nomiya, *Inorganic chemistry*, 2003, **42**, 8028

32. M. Montazer, F. Alimohammadi, A. Shamei, M. K. Rahimi, *Colloids and Surfaces B: Biointerfaces*, 2012, **89**, 196

33. A. Koski, K., Yim, S. Shivkumar, *Materials Letters*, 2004, **58,** 493

34. M. S. Islam, M. R. Karim, *Colloids and Surfaces A: Physicochemical and Engineering Aspects*, 2010, **366**, 135

35. C. C. DeMerlis, D. R. Schoneker, *Food and Chemical Toxicology*, 2003, 41, 319

36. E. Shoba, R. Lakra, M. S. Kiran and P. S. Korrapati, *RSC Adv*., 2014, **4**, 60209

37. M. H. El-Naas, S. Al-Zuhair, S. Makhlouf, *Journal of Industrial and Engineering Chemistry*, 2010, **16**, 267

38. J. H. Park, M. R. Karim, I. K. Kim, I. W. Cheong, J. W. Kim, D. G. Bae, J. H. Yeum, *Colloid and Polymer Science*, 2010, **288**, 115

39. Y. You, C. Zhang, *Journal of Clinical Rehabilitative Tissue Engineering Research*, 2010, **16**, 5498

40. M. J. Hajipour, K. M. Fromm, A. A. Ashkarran, D. J. de Aberasturi, I. R. de Larramendi, T. Rojo, M. Mahmoudi, *Trends in biotechnology*, 2012, **30**, 499

41. K. Zhou, S. Jiang, C. Bao, L. Song, B. Wang, G. Tang, Y. Hu, Z. Gui, *RSC Adv*., 2012, **2**, 11695

42. A. G. Destaye, C. K. Lin, and C. K. Lee, *ACS Appl. Mater. Interfaces*, 2013, **5**, 4745

43. H. S. Mansur, C. M. Sadahira, A. N. Souza, A. A. Mansur, *Materials Science and Engineering: C*, 2008, **28**, 539

44. H. S. Mansur, C. M. Sadahira, A. N. Souza, A. A. P. Mansur, *Mater. Sci. Eng., C*, 2008, **28**, 539

45. S. Jiang, G. Duan, E. Zussman, A. Greiner, S. Agarwal, *ACS applied mater. Interfaces,* 2014, **6**, 5918

46. B. Zhang, S. Xu, H. Tang and P. Wu, *RSC Adv*., 2013, **3**, 8372

47. M. Li, S. Cheng and H. Yan, *Green Chem*., 2007, **9**, 894

48. S. I. Torigoe, T. Horikoshi, A. Ogawa, T. Saito, T. Hamada, *Journal of Advanced Concrete Technology*, 2003, **1**, 265

49. D. Lee, R. E. Cohen, M. F. Rubner, *Langmuir*, 2005, **21**, 9651